Afterloader integrated EMT enables improved dwell position model definition and quality assurance in Venezia gynaecological brachytherapy applicators

Androulakis, Ioannis; van Laar, Myra; Godart, Jeremy; Straathof, Robin; Westerveld, Henrike; Nout, Remi; Hoogeman, Mischa; Kolkman-Deurloo, Inger Karine K.

DOI
10.1088/1361-6560/addfa7

Publication date
2025

Document Version
Final published version

Published in
Physics in medicine and biology

Citation (APA)
Androulakis, I., van Laar, M., Godart, J., Straathof, R., Westerveld, H., Nout, R., Hoogeman, M., & Kolkman-Deurloo, I. K. K. (2025). Afterloader integrated EMT enables improved dwell position model definition and quality assurance in Venezia gynaecological brachytherapy applicators. *Physics in medicine and biology*, *70*(12), Article 125003. https://doi.org/10.1088/1361-6560/addfa7

Physics in Medicine & Biology

PAPER • OPEN ACCESS

Afterloader integrated EMT enables improved dwell position model definition and quality assurance in Venezia gynaecological brachytherapy applicators

To cite this article: Ioannis Androulakis *et al* 2025 *Phys. Med. Biol.* **70** 125003

IOP Publishing Phys. Med. Biol. 70 (2025) 125003 https://doi.org/10.1088/1361-6560/addfa7

Physics in Medicine & Biology

IPEM Institute of Physics and Engineering in Medicine

OPEN ACCESS

RECEIVED
7 February 2025

REVISED
14 May 2025

ACCEPTED FOR PUBLICATION
2 June 2025

PUBLISHED
10 June 2025

PAPER

Afterloader integrated EMT enables improved dwell position model definition and quality assurance in Venezia gynaecological brachytherapy applicators

Ioannis Androulakis[1,*], **Myra van Laar**[1], **Jeremy Godart**[1,2], **Robin Straathof**[1,3], **Henrike Westerveld**[1], **Remi Nout**[1], **Mischa Hoogeman**[1,2] and **Inger-Karine K Kolkman-Deurloo**[1]

[1] Department of Radiotherapy, Erasmus MC Cancer Institute, University Medical Center, Rotterdam, The Netherlands
[2] Department of Medical Physics and Informatics, HollandPTC, Delft, The Netherlands
[3] Department of BioMechanical Engineering, Delft University of Technology, Delft, The Netherlands
[*] Author to whom any correspondence should be addressed.

E-mail: i.androulakis@erasmusmc.nl

Keywords: cervical cancer, brachytherapy, applicator reconstruction, electromagnetic tracking, quality assurance

Abstract

Objective. In brachytherapy for gynecological cancers using intracavitary applicators, implant reconstruction is commonly performed using applicator libraries. These libraries contain applicator geometry models as well as dwell position (DP) models defined in respect to the applicator geometry. In this study, we investigate whether an afterloader integrated electromagnetic tracking (EMT) system can be utilized for DP model definition and quality assurance in such applicators. *Approach.* DPs in four sets of two configurations of the Elekta Venezia Advanced Gynaecological Applicator (22 mm ovoids/40 mm intrauterine (IU) and 26 mm ovoids/70 mm IU) were measured using an afterloader integrated EMT system. Measurements were evaluated for reproducibility and compared against manufacturer-specified (MS) DPs and a computed tomography (CT)-corrected DP model. *Main Results.* Excellent EMT measurement reproducibility was observed, with values of $\leqslant$0.2 mm for both configurations. The overall reproducibility, including applicator geometry reproducibility, was $\leqslant$0.4 mm for both configurations. Significant discrepancies from the manufacturer's DP model were observed, with a mean $\pm$ sd deviation of 1.13 ± 0.66 mm (22/40) and 1.37 ± 0.63 (26/70), particularly in the IU channel, where MS DPs were not experimentally defined. Discrepancies were reduced to 0.89 ± 0.41 mm (22/40) and 0.81 ± 0.33 mm (26/70) when the CT-corrected DP model was used as baseline, highlighting the need for experimentally defined DP models. The overall uncertainty of single measurements was below the clinically acceptable 2 mm limit. *Significance.* This study confirms that afterloader integrated EMT can accurately reconstruct source paths in gynecological brachytherapy applicators and supports its incorporation into clinical workflows for improved quality assurance and treatment precision. The importance of EMT for quality assurance was highlighted by measured deviations from manufacturer's DP model in a clinical relevant part of the IU channel.

1. Introduction

Brachytherapy (BT) is an established treatment option for gynecological cancers (Holschneider *et al* 2019). In this type of treatment, implanted intracavitary applicators with or without interstitial needles are used to guide a radioactive source to predetermined dwell positions (DPs) for predetermined dwell times using an afterloader. The DPs and times are optimized to achieve a conformal dose distribution in the target, while sparing surrounding organs at risk as much as possible. As BT is characterized by a steep dose gradient, $<$2 mm accuracy in the reconstruction of these implants and their associated DPs with respect to patient anatomy is of great importance (Siebert *et al* 2020, Prisciandaro *et al* 2022). Quality assurance (QA) and pre-treatment verification of the reconstruction are, therefore, essential to ensure accurate dose delivery.

Among other methods (Espinoza *et al* 2013, Watanabe *et al* 2018, Lekatou *et al* 2022, van Wagenberg *et al* 2024), electromagnetic tracking (EMT) has been proposed as a QA tool for pre-treatment verification of the implant reconstruction (Sauer *et al* 2022). Compared to other techniques, EMT has the advantage that it can provide three dimensional information with sub-millimetre accuracy without a line of sight, and that implant QA is performed before rather than during irradiation.

In EMT the position and orientation of a small sensor is tracked in 3D space (Franz *et al* 2014). The sensor is localized by measuring the magnetic flux in a varying magnetic field with a known geometry created by a field generator. Although EMT is limited to a tracking volume within which the magnetic field geometry is defined and is sensitive to electromagnetic disturbances, the small sensor size, lack of line-of-sight restrictions, and submillimeter accuracy make EMT suitable for brachytherapy pre-treatment verification (Franz *et al* 2014, Dürrbeck *et al* 2022a). Specific applications of EMT in the brachytherapy workflow include navigation during needle implantation, reconstruction error detection, and implant reconstruction (Damato *et al* 2014, Bert *et al* 2016, Beaulieu *et al* 2018, Dürrbeck *et al* 2022b, Deufel *et al* 2024, Gomez-Sarmiento *et al* 2024). The potential application of EMT in brachytherapy has been further facilitated by the development of a prototype afterloader-integrated EMT system that can drive an EMT sensor integrated in the check cable through the DPs in the implants, enabling seamless integration of EMT in the brachytherapy workflow (Kallis *et al* 2018). In particular, this technology demonstrated high potential in phantoms and could therefore be utilized during commissioning and regular QA of brachytherapy applicator geometry and source path (Dürrbeck *et al* 2024).

The accuracy of EMT measurements using the afterloader-integrated EMT system was found sufficient for quality assurance of the interstitial needles (Kellermeier *et al* 2017, van Heerden *et al* 2021, Dürrbeck *et al* 2024). The system has been clinically investigated as a quality assurance tool for interstitial implants in breast, prostate, as well as cervical BT treatments (Kallis *et al* 2019, Kolkman-Deurloo *et al* 2022, Androulakis *et al* 2024, Androulakis *et al* 2025). For gynecological brachytherapy, also a workflow for EMT-based interstitial needle reconstruction using applicator-based registration to the imaging coordinate system has been proposed (Gomez-Sarmiento *et al* 2024).

Defining the accuracy of EMT-based reconstruction of the source path in gynecological applicators, consisting of intrauterine (IU) and ovoid or ring channels, is more challenging than for interstitial needles. EMT measured DPs showed deviations from the manufacturer specified (MS) DP model up to 2.4 mm in channels of the Utrecht cervical applicator (Elekta AB, Stockholm, Sweden) (van Heerden *et al* 2021). The reason for these deviations is not yet clear, and it is not certain that the MS DP models in the applicator libraries of the treatment planning system represent the true source paths of these channels. Several studies have found significant differences between own measured DPs in gynecological applicators using two-dimensional techniques (such as physical measurements, gafchromic film, and radiographic techniques) and the respective MS DP model clinically used in the applicator library of the treatment planning system (Awunor *et al* 2013, 2015, Otani *et al* 2018). The applicator channels have a higher curvature and a wider lumen diameter than interstitial needles, which increases curving and snaking effects (Hellebust *et al* 2010, Niatsetski *et al* 2011, Straathof *et al* 2024). Furthermore, manufacturing tolerances in the applicator geometry may lead to deviations from the MS DPs (Awunor *et al* 2015, Humer *et al* 2015). On the other hand, differences in geometry and mechanical characteristics of source and EMT sensor cables may result in deviations between actual and EMT measured source paths, in particular for channels with larger lumens and higher curvatures, owing to the differences in size and geometry of the source and the EMT sensor and the cable mechanical characteristics of both devices. Therefore, before using EMT measurements in clinical applications for IU and ovoid/ring channels, measurements that accurately represent the true source positions are necessary.

The aim of this study is to report the reproducibility and accuracy of EMT when measuring the source positions in the Venezia Advanced Gynaecological Applicator (Elekta AB, Stockholm, Sweden). Several steps were performed to this end. First, the reproducibility of the EMT measurements was evaluated for two different applicator configurations. Subsequently, the applicator geometry reproducibility of four different sets of each applicator configuration was evaluated. The mean EMT-measured positions were then compared to the MS DP model. To handle potential uncertainties of the MS DP model, 3D DPs were acquired using computed tomography (CT) at each source position, and a CT-corrected DP model (CT DP) was created to evaluate both the EMT measurements and the MS DP model.

2. Materials and methods

2.1. Venezia applicators and QA phantom

Venezia Advanced Gynecological Applicators (Elekta AB, Stockholm, Sweden) were used in our analysis. The Venezia applicator consists of three applicator channels and allows for interstitial needle insertion

(figure 1(a)). The central channel is an IU channel with variable length and angle. The other two channels comprise two hemispherical (lunar) ovoids with variable diameters and a fixed ovoid-plane rotation of 60°. All three channels are individual components that can be assembled in a fixed single applicator configuration. Two different applicator configurations were used in this study. The first applicator configuration (26/70) consisted of a 70 mm/30° IU channel with two 26 mm/60° ovoids. The second configuration (22/40) consisted of a 40 mm/30° IU channel with two 22 mm/60° ovoids. In both configurations, the ovoid plane is perpendicular to the IU channel. Four different sets were available for each configuration. Two sets of each configuration were at their end of life (three years of use), just before being phased out of the clinical workflow. The other two sets of each configuration were new applicators immediately after being commissioned for and accepted in the clinical workflow. All applicators had a manufacturer-reported geometrical deviation tolerance of ± 1 mm until their end of life.

For the measurements, a CT- and EMT-compatible QA phantom (PTBV phantom, Elekta AB, Stockholm, Sweden), as has been previously described (Dürrbeck *et al* 2024, Gomez-Sarmiento *et al* 2024), was used. The Venezia applicators were fixated to the phantom using an integrated fixation clamp (figure 1(b)).

2.2. EMT afterloader prototype and measurement protocol

A Flexitron afterloader prototype (Elekta AB, Stockholm, Sweden) with a custom 5-degree-of-freedom EMT sensor integrated in the check cable drive, connected to an Aurora V3 EMT system (Northern Digital Inc., Waterloo, ON Canada), was used in this study (Kallis *et al* 2018). The sensor (shown in figure 1(c)) can follow predefined DPs that mimic the source path. The system records the sensor position and orientation with a refresh rate of 40 Hz within the cubic measurement volume of the EMT field generator. The manufacturer reported accuracy of the EMT sensor is 1.4 mm ($k = 2$, i.e. a coverage factor of 2 as to define a 95.4% confidence interval). The source cable drive of this prototype device was loaded with a non-radioactive dummy source capsule identical to the 192-Ir Flexisource, which will be referred to as the source in the rest of the document. Both the EMT and the source cable insertion depths were calibrated prior to the experimental procedure (Steenhuijsen *et al* 2018).

The EMT measurements were performed along the entire length of each of the three applicator channels with 5 mm steps using forward stepping (towards the tip of each channel). The sensor was stationed for 3 s at each position, and excluding the first 10 measurements (first 0.25 s), the average coordinates were recorded following the protocol of Durrbeck *et al* (2024). Measuring 3 s per DP ensured that a minimum of 100 samples were obtained at each DP, at which measurement jitter is minimized (Dürrbeck *et al* 2024). All the measurements were performed in an electromagnetic-interference-free environment. Raw measurement data are made publicly available at (Androulakis 2025).

2.3. Manufacturer specified DP model

MS DPs in the ovoid channels are based on measurements by the manufacturer using a radiographic simulator (Niatsetski *et al* 2011, Steenhuijsen *et al* 2018). DPs from depth 215 mm until the tip (300 mm) of the ovoid channels are available in the MS DP model. The MS DPs in the IU channel, however, are specified on the centreline of the IU channel model along the whole length(from depth 51 mm to 300 mm), but not based on measurements. The manufacturer chose to perform measurements only for the channels with very steep curvature (Elekta Brachytherapy 2018). The DP geometry of both applicator configurations can be seen in figures 1(d) and (e).

2.4. CT-corrected applicator DP model

Because the MS DPs in the IU were not experimentally defined, the DPs of this channel were measured using 3D CT images. Since the MS DPs in the ovoid channels were already experimentally defined, additional model correction was not regarded necessary in those channels. CT imaging was performed on a Somatom Confidence scanner (Siemens Healthineers, Erlangen, Germany) with 120 kVp and 18 mA tube voltage and current settings, with a spatial resolution of 0.32 mm in the axial plane, and a slice thickness of 0.5 mm. The applicator was fixed to the QA phantom, connected to the afterloader prototype using transfer tubes, and positioned in the CT scanner such that the IU channel is positioned parallel to the sagittal plane of the scanning coordinates (figure 2). Images were made while positioning the source at DPs spaced 10 mm apart between 210 mm and 300 mm (the most distal position) in the channel. Each DP was determined by positioning a point marker in the centre of the visible source capsule using MIM (MIM Software, Cleveland, OH, USA). The DP model was adapted using a linear interpolation of the CT measured DPs in the IU channel, resulting in the CT DP model.

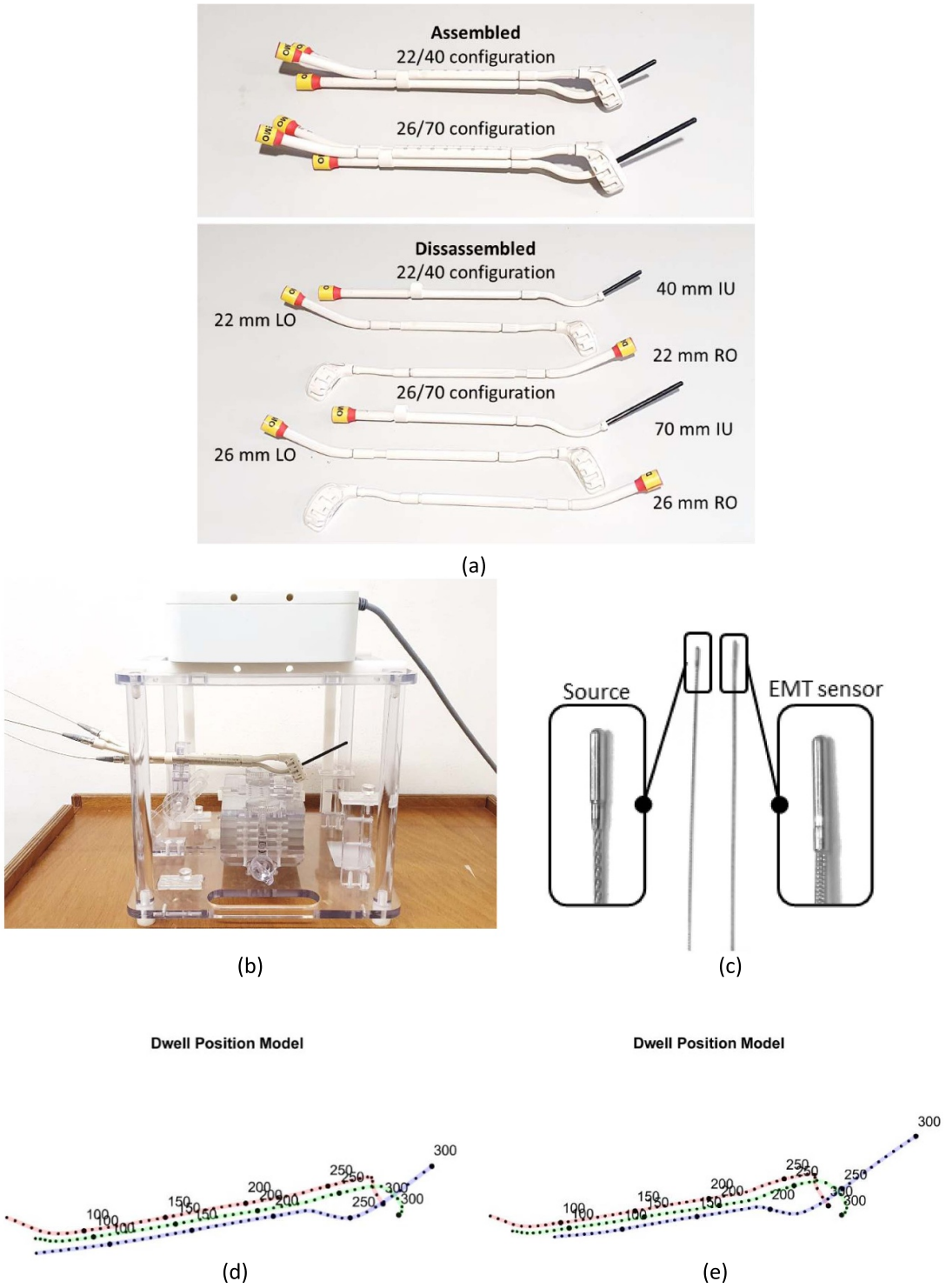

Figure 1. (a) Venezia applicator configurations used in this study, (b) 26/70 applicator positioned on the QA phantom for EMT measurement. (c) Afterloader integrated EMT sensor and source capsule. (d) Dwell position (DP) model geometry in the 22/40 applicator configuration. (e) DP model geometry in the 26/70 applicator configuration. Right ovoid DP model is marked red, left ovoid DP model is marked green, intrauterine channel DP model is marked blue.

2.5. Uncertainty analysis

The uncertainty analysis was performed in line with recommendations by GEC-ESTRO, AAPM, and NIST (Taylor and Kuyatt 1994, DeWerd *et al* 2011, Kirisits *et al* 2014). The overall applicator measurement reproducibility (Type A uncertainty) was assumed to be a combination of two independent factors: the reproducibility of each individual EMT measurement in the same applicator (s_{EMT}), and the geometric reproducibility of each applicator ($s_{\mathrm{applicator}}$). The overall reproducibility was calculated as:

$$s_{\mathrm{total}} = \sqrt{{s_{\mathrm{EMT}}}^2 + {s_{\mathrm{applicator}}}^2} \quad . \tag{1}$$

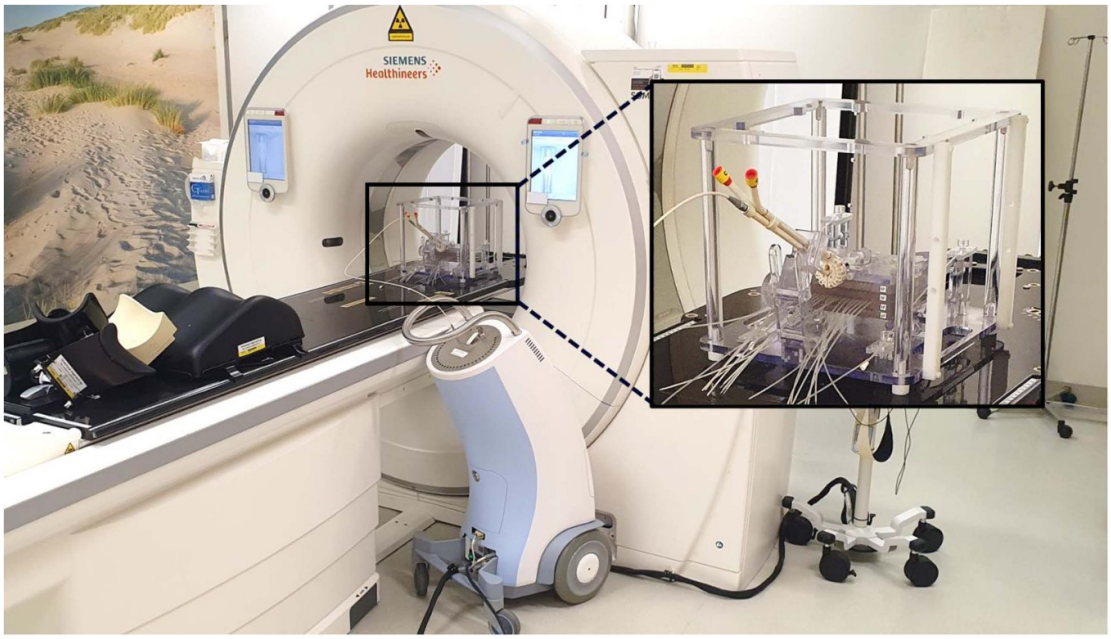

Figure 2. Experimental setup for CT-based DP determination in the intrauterine channel of a 26/70 Venezia applicator configuration, using the QA phantom. The intrauterine channel is connected to the EMT integrated Flexitron afterloader prototype device.

For each applicator configuration set, 5 EMT measurements were performed. Between measurements, the sets were repositioned on the QA phantom and reconnected to the afterloader prototype, to avoid the introduction of setup-specific bias.

For the calculation of the EMT measurement reproducibility (s_{EMT}), we used repeated experiments in a single applicator, hence maintaining the geometry stable. The EMT measured DPs of each set were registered to the DPs of the initial measurement using the Procrustes transformation between corresponding DPs as implemented in MATLAB R2023a (Mathworks, Natick, MA, USA) (Sauer *et al* 2024). To prevent the deformation of the true geometry of the implant, scaling as well as reflection in the Procrustes transformation were disabled. The EMT measurement reproducibility (s_{EMT}) was calculated as:

$$s_{\mathrm{EMT}} = \sqrt{\frac{\sum_{k=0}^{p}\sum_{j=0}^{n}\sum_{i=0}^{m}\left(r_{i,j,k}-\overline{r_{j,k}}\right)^2}{mnp}} \tag{2}$$

where $r_{i,j,k}$ is the registered position of the ith measurement of the jth DP of the kth applicator configuration set, $\overline{r_{j,k}}$ is the mean registered position of the jth DP of the kth applicator configuration set, and m, n, p, are the number of measurements, DPs, and applicator configuration sets, respectively.

For the calculation of the applicator geometry reproducibility ($s_{\mathrm{applicator}}$), we used the mean measurement derived from multiple measurements of each applicator to eliminate the influence of the EMT measurement reproducibility. The mean registered EMT DPs $\overline{r_{j,k}}$ of each applicator configuration set were calculated, creating an EMT DP model of each applicator configuration set. Again, the EMT DP models of each applicator configuration set were registered to the DPs of the initial applicator configuration set, calculating the geometric reproducibility of each applicator configuration ($s_{\mathrm{applicator}}$) as:

$$s_{\mathrm{applicator}} = \sqrt{\frac{\sum_{k=0}^{p}\sum_{j=0}^{n}\left(\overline{r'_{j,k}}-\overline{r'_{k}}\right)^2}{np}} \tag{3}$$

where $\overline{r'_{j,k}}$ is the registered position of the jth DP of the kth applicator configuration set in the EMT DP model of each applicator configuration set.

The mean registered EMT DP model positions $\overline{r'_{k}}$ of each applicator configuration were calculated, creating an EMT DP model of the applicator configuration.

For the calculation of accuracy (Type B uncertainty), the mean EMT DPs were registered to the available DPs in the MS DP or CT DP model. The registration was performed using the Procrustes transformation between corresponding DPs. Scaling as well as reflection in the Procrustes transformation were disabled. The mean Euclidean distance between corresponding EMT DP model and MS DP or CT DP model was used for overall accuracy (u) definition.

The overall uncertainty (V) was calculated as the combination of reproducibility and accuracy, calculated as:

$$V = k\sqrt{s_{\text{total}}{}^2 + u^2} \quad . \tag{4}$$

In the calculations of overall uncertainty a coverage factor of 2 was used ($k = 2$) to approximate a 95% level of confidence, while a coverage factor of 1 ($k = 1$) was used for all partial uncertainties, such as the reproducibility, as is recommended and followed in the GEC-ESTRO, AAPM, and NIST guidelines (Taylor and Kuyatt 1994, DeWerd *et al* 2011, Kirisits *et al* 2014).

3. Results

3.1. Reproducibility

The measurement reproducibility s_{EMT} was 0.14 mm and 0.16 mm for the 22/40 and 26/70 configuration, respectively. The measurement reproducibility per DP is shown in figures 3(a) and (b), for the 22/40 and 26/70 configuration, respectively. The measurement reproducibility was slightly lower at the most proximal DPs of the left ovoid (LO), before the transition to the RO curve for the 22/40 configuration, and at the distal end of the ovoid channels, although it stayed lower or equal to 0.3 mm in all DPs.

The applicator geometry reproducibility $s_{\text{applicator}}$ was 0.30 mm and 0.32 mm for the 22/40 and 26/70 configuration, respectively. The applicator geometry reproducibility per DP is shown in figures 4(a) and (b), for the 22/40 and 26/70 configuration, respectively. The applicator geometry reproducibility was lower at the proximal DPs of the 22/40 configuration, which do not have a clinical function. The Applicator geometry reproducibility was also lower at the most distal DPs in the ovoids in both configurations. Moreover, the applicator geometry reproducibility was relatively lower along the whole length of the IU channel of the 26/70 configuration.

Overall reproducibility, calculated according to equation (1) was 0.33 mm and 0.36 mm for the 22/40 and 26/70 configuration, respectively.

3.2. Deviations from MS DP model

Deviations per DP are shown in figures 5(a) and (b) for the 22/40 and 26/70 configuration, respectively. Deviations of the EMT DP model from the MS DP model had a mean ± sd of 0.94 ± 0.60 mm and 1.12 ± 1.26 mm for the 22/40 and 26/70 configuration, respectively. Including only the clinically relevant DPs 215 mm to 300 mm, these values were 1.13 ± 0.66 mm and 1.37 ± 0.63 mm for the 22/40 and 26/70 configuration, respectively. Looking only at the DPs in the ovoids, mean ± std deviation was 0.94 ± 0.60 mm and 0.91 ± 0.37 mm for the 22/40 and 26/70 configuration, respectively. Looking only at the DPs 210 mm to 300 mm for the IU channel, mean ± sd deviation was 1.52 ± 0.87 mm and 1.88 ± 0.70 mm for the 22/40 and 26/70 configuration, respectively. High deviations in the IU channel in both applicator configurations, especially in the distal part (i.e. tip), were observed.

Separate radial and longitudinal deviations of the EMT DP model from the MS DP model are shown in figures 5(c) and (d) (radial) and figures 5(e) and (f) (longitudinal) for the 22/40 and 26/70 configuration, respectively. The mean ± std radial deviation was 0.80 ± 0.59 mm and 0.95 ± 0.61 mm for the 22/40 and 26/70 configuration, respectively. The mean ± std longitudinal deviation was 0.13 ± 0.48 mm and 0.14 ± 0.60 mm for the 22/40 and 26/70 configuration, respectively.

3.3. Experimentally defined DPs in IU channel

Figures 6(a) and (b) show sagittal CT images of the source and EMT sensor, respectively, at the most distal DP (i.e. tip) in the 70 mm IU channel. Figure 6(c) shows the annotated source and EMT sensor DPs in the CT image of the IU channel. The source and EMT sensor DPs align well with each other, while following the outer curve of the channel, rather than the centreline of the channel. The differences between EMT sensor, source, and MS DP model (thus centreline) for each annotated DP can be seen in figure 6(d). For the 40 mm IU channel, the mean ± sd difference between source and EMT sensor DPs was 0.25 ± 0.17 mm, while their mean ± sd difference from the MS DP model (thus centreline) was 0.77 ± 0.34 mm and 0.84 ± 0.38 mm for the source and EMT sensor, respectively. Similarly for the 70 mm IU channel, the mean ± sd difference between source and EMT sensor DPs was 0.30 ± 0.19 mm, while their mean ± sd difference from the MS DP model (thus centreline) was 1.42 ± 0.36 mm and 1.31 ± 0.30 mm for the source and EMT sensor, respectively.

3.4. Deviation from CT-corrected DP model

Deviations per DP are shown in figures 7(a) and (b). Deviations of the mean EMT measured 22/40 and 26/70 applicator model from the CT DP model had a mean ± sd of 0.89 ± 0.41 mm and 0.81 ± 0.33 mm,

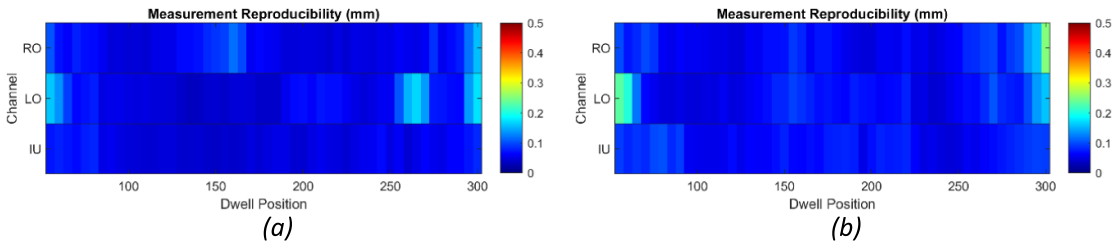

Figure 3. Measurement reproducibility s_{EMT} per DP of (a) the 22/40 applicator configuration, and (b) the 26/70 applicator configuration. On the left and right side of the horizontal axis are the most proximal and most distal evaluated DP in each channel, respectively. RO: right ovoid channel, LO: left ovoid channel, IU: intrauterine channel.

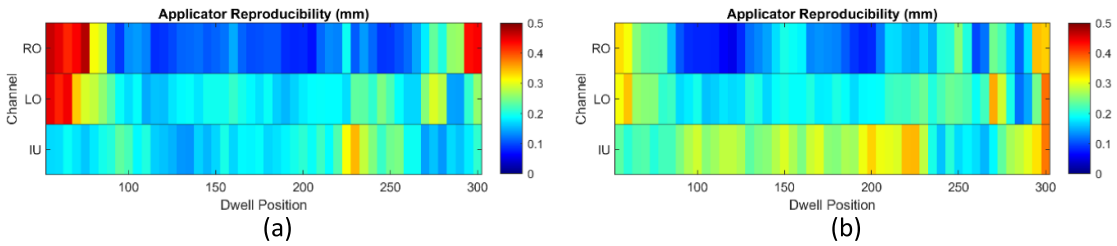

Figure 4. Applicator reproducibility $s_{geometry}$ per DP of (a) the 22/40 applicator configuration, and (b) the 26/70 applicator configuration. On the left and right side of the horizontal axis are the most proximal and most distal evaluated DP in each channel, respectively. RO: right ovoid channel, LO: left ovoid channel, IU: intrauterine channel.

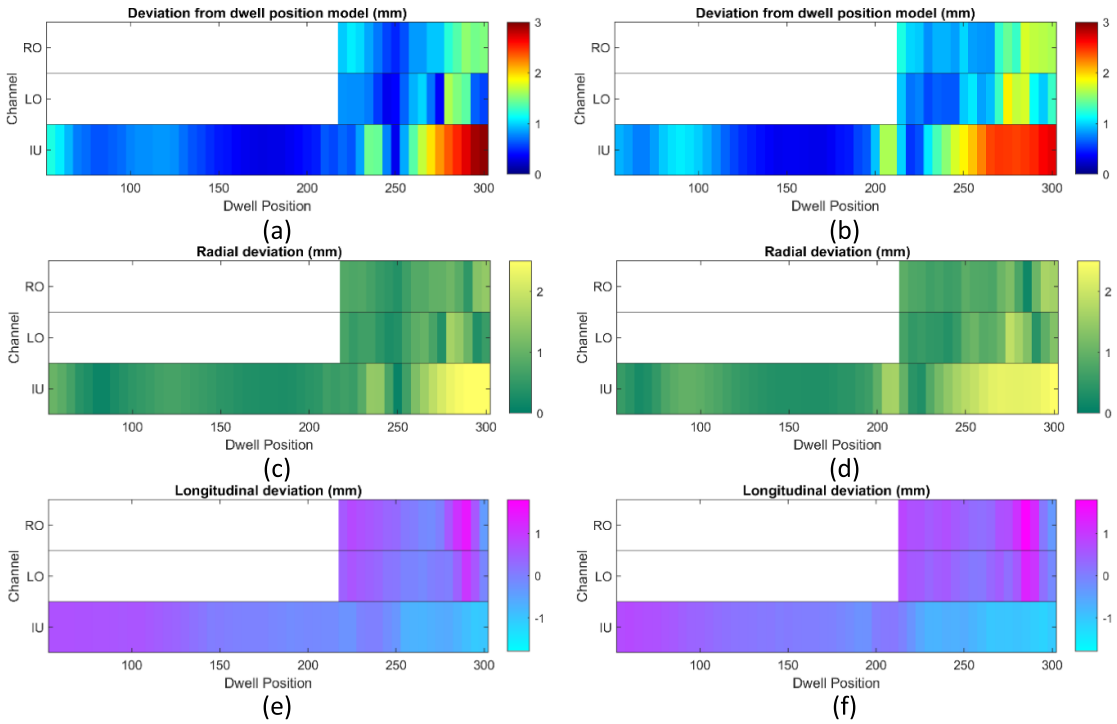

Figure 5. Deviation from DP model per DP of (a) the 22/40 applicator configuration, and (b) the 26/70 applicator configuration. Radial part of the deviation from the DP model per DP of (c) the 22/40 applicator configuration, and (d) the 26/70 applicator configuration. Longitudinal part of the deviation from the DP model per DP of (e) the 22/40 applicator configuration, and (f) the 26/70 applicator configuration. In the latter graphs, negative values represent a delay of the measured points along the channel path. On the left and right side of the horizontal axis are the most proximal and most distal evaluated DP in each channel, respectively. RO: right ovoid channel, LO: left ovoid channel, IU: Intrauterine channel.

respectively. Looking only at the DPs in the ovoids, mean $\pm$ sd deviation was 0.85 $\pm$ 0.34 mm and 0.81 $\pm$ 0.38 mm, respectively. Looking only at the DPs of the IU channel, mean $\pm$ sd deviation was 0.96 $\pm$ 0.52 mm and 0.81 $\pm$ 0.21 mm, respectively.

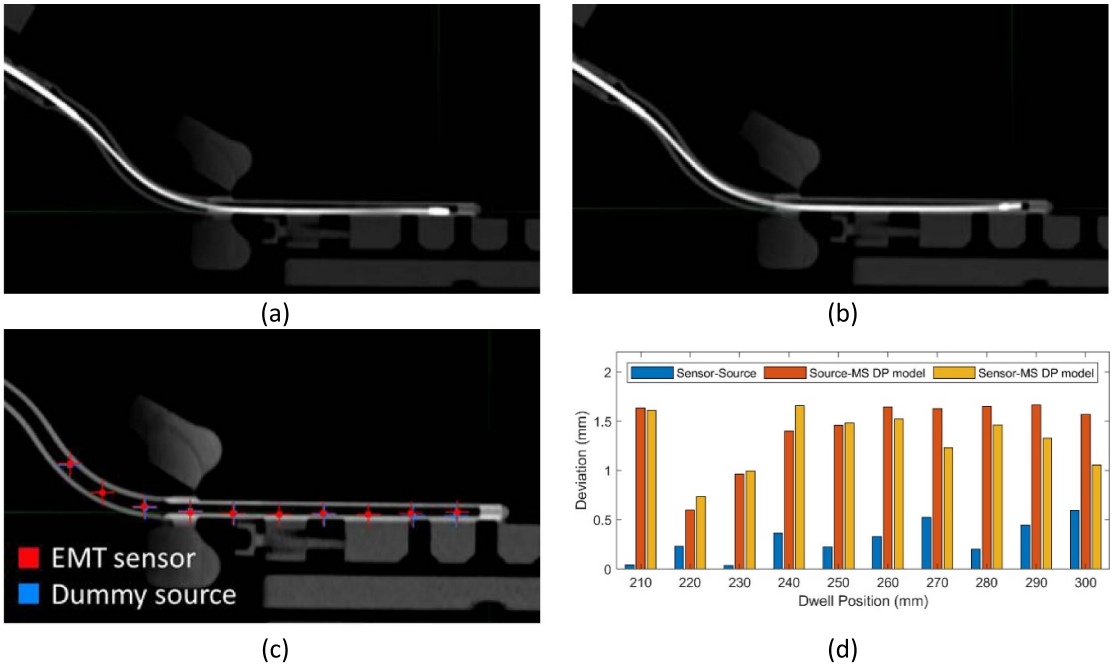

Figure 6. CT based analysis of the EMT sensor and source DPs in the 70 mm IU. Sagittal CT images along the centre of the intrauterine channel (a) while the source is on the most distal DP, (b) while the EMT sensor is on the most distal DP, (c) showing the annotated DPs of the EMT sensor and the source in red and blue, respectively. (d) Recorded deviation of annotated and model MS DPs.

Separate radial and longitudinal deviations of the EMT DP model from the CT DP model are shown in figures 7(c) and (d) (radial) and figures 7(e) and (f) (longitudinal) for the 22/40 and 26/70 configuration, respectively. The mean $\pm$ std radial deviation was 0.72 $\pm$ 0.43 mm and 0.66 $\pm$ 0.35 mm for the 22/40 and 26/70 configuration, respectively. The mean $\pm$ std longitudinal deviation was 0.14 $\pm$ 0.50 mm and 0.08 $\pm$ 0.45 mm for the 22/40 and 26/70 configuration, respectively.

It can be appreciated in figures 7(g) and (h) that there is a better agreement between EMT measurements and DP model with the addition of the CT based source positions not only in the IU channel, but to a lesser extent also in the ovoid channels, due to better registration of the two DP models.

3.5. Overall uncertainty

Based on the previous results, the overall uncertainty ($k = 2$) according to equation (2) is 1.82 mm and 1.91 mm, when comparing EMT to the CT corrected applicator DP model of the 22/40 and 26/70 configuration, respectively.

4. Discussion

In this study we evaluated the accuracy and reproducibility of afterloader integrated EMT in the intracavitary channels of Venezia applicators. Firstly, we found an excellent measurement reproducibility of $\leqslant$0.2 mm, although the lumen diameter of the applicator would theoretically allow for freedom of movement within the channels. The determined applicator geometry reproducibility of $\leqslant$0.3 mm was well within the manufacturer's specifications. Secondly, we found that the deviation between the EMT DP model and the MS DP model was around 1.0 $\pm$ 0.5 mm. This deviation was especially high in the IU channel for both evaluated applicator configurations. Thirdly, we found that the sensor and source follow a similar physical path, which deviates from the centreline of the IU channel. Fourthly, EMT measurements agreed substantially better with the CT DP model, leading to an accuracy of $<$1 mm, and an overall uncertainty of $<$2 mm for a single EMT measurement.

In earlier research, Dürrbeck *et al* found good reproducibility of an intracavitary gynecological ring applicator geometry where maximum EMT measurement deviations of positions in the ring and IU were 0.33 mm and 0.25 mm, respectively (2024). Our reproducibility of 0.14 mm and 0.16 mm for the 22/40 and 26/70 configurations of the Venezia applicator, align well with these results. In the study of van Heerden *et al*, deviations of up to 2.4 mm were found when comparing EMT measurements with the DP model in a Utrecht CT/MR applicator (2021). These results are similar to our current findings, where deviations from

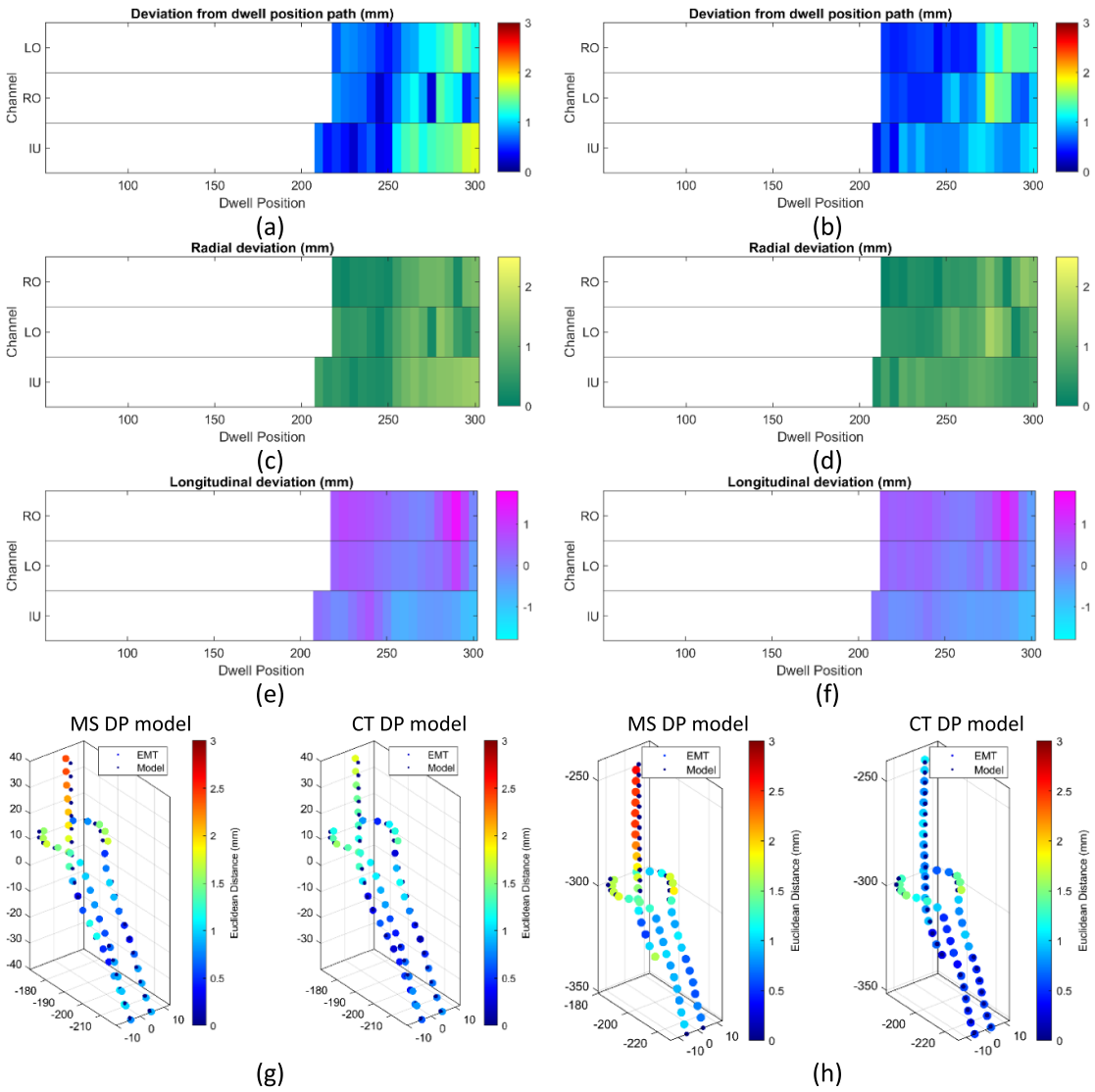

Figure 7. (a)–(f) Deviation from corrected CT DP model per DP of the (a) 22/40 and (b) 26/70 applicator configuration. Radial part of the deviation from the DP model per DP of (c) the 22/40 applicator configuration, and (d) the 26/70 applicator configuration. Longitudinal part of the deviation from the DP model per DP of (e) the 22/40 applicator configuration, and (f) the 26/70 applicator configuration. In the latter graphs, negative values represent a delay of the measured points along the channel path. On the left and right side of the horizontal axis are the most proximal and most distal evaluated DP in each channel, respectively. RO: right ovoid channel, LO: left ovoid channel, IU: Intrauterine channel. (g), (h) Three-dimensional representation of the EMT measurements registered to the manufacturer-specified DP model on the left, and the corrected CT DP model on the right for the (g) 22/40 and (h) 26/70 applicator configuration. Colours of the EMT DPs show the Euclidean distance from the model.

the MS DP model were up to 2.9 mm (figure 5). We identified that the largest errors were in the IU channel, where the MS DP model is based on the centreline of the IU channel. Similar results can be observed in the measurements by Gomez-Sarmiento *et al*, where EMT measured DPs of the ring gynecological applicator seem to deviate from the centreline in the IU channel (2024).

Reproducibility was in some instances worse in the most distal and most proximal edges of the applicator. We took measures to minimize the likeliness that such discrepancies would be created due to distortions of the electromagnetic field generated by the field generator. Namely, we tried to eliminate positioning bias by repositioning the applicator between measurements. We also made sure the applicator is positioned centrally in the measurement volume, where the EMT system manufacturer reports the highest system accuracy. Finally, we made sure that the most clinically relevant distal parts were in the centre of the field. Given the fact that the most distal and most proximal parts of the applicator coincide with higher curvature, it can be assumed that the slightly worse reproducibility is created due to increased freedom of movement and snaking effect due to the curvature.

With measurement reproducibility well within submillimeter and an overall measurement uncertainty <2 mm, afterloader integrated EMT can be utilized for applicator geometry deformation detection.

Afterloader integrated EMT can thus be used for periodic QA checks during the expected service life, to check whether the required geometrical accuracy of ±1 mm is maintained (Hellebust *et al* 2010, Steenhuijsen *et al* 2018). This could be achieved by comparing periodically acquired measurements with an initial measurement during commissioning of the applicator. With afterloader integrated EMT measurements this can be performed reproducibly, faster, and more efficiently than with CT, grafchromic or radiographic techniques. For commissioning of the applicators it is recommended to accompany EMT measurements by CT imaging, since the DP model, whilst reproducible, deviates from the tube centreline due to cable curving and snaking. Based on our findings we suggest a minimum agreement tolerance of 2 mm between expected and measured DPs.

Our findings from the CT images revealed similar mechanical behaviour within the relatively wide lumen of the applicator, with the physical DPs of the EMT sensor and the source being well-aligned. However, these CT-based and EMT-based DPs deviate significantly from the MS DP model (which is centreline based in the IU channel). When we compared the EMT measurements with the CT corrected DP model, which includes CT-based positions for the IU channel, we found an accuracy of <1 mm. This adapted DP model is based on point annotations and reconstructions on imaging data, which have an expected interobserver variability around 0.8 ± 0.3 mm, according to Hrinivich *et al* (Hrinivich *et al* 2019). Taking this into account, the real accuracy of EMT measurement-derived DPs is likely lower. EMT-derived DPs provide a more accurate prediction of the source path than the tube centreline, although any more accurate methods for DP model acquisition should be recommended if such technology is available.

In Gomez-Sarmiento *et al*, a method was proposed for EMT-based needle reconstruction in gynecological treatments with both applicators and needles. The method was based on an accurate registration of the EMT measurements to the applicator DP model (2024). In the same study, implant reconstruction accuracy was found to be <2 mm. With an overall uncertainty of <2 mm observed in this study, this is a logical result. Given our results, applicator based registration should be performed only using channels where a measured DP model is available. For the Venezia applicator, we recommend this type of EMT-based reconstruction therefore to only use the ovoid channels, unless a measured DP model for the IU channel is provided.

In conclusion, we have demonstrated the reliability of EMT to reconstruct the DP model of Venezia gynecological applicators. We observed that DP measurements are accurate and reproducible, and that the EMT sensor follows a similar physical path as the source. However, our analysis has also revealed the limitations of the currently provided MS DP model. In this context, EMT emerges as a potential candidate for providing a more accurate DP model than centreline data. The role of EMT extends beyond this, finding relevance in the commissioning process, where it could be utilized in combination with CT, and in the execution of periodic applicator QA. The proposal of EMT-based implant reconstruction by Gomez-Sarmiento appears feasible also for Venezia applicators, and could be improved using EMT- or CT-based applicator DP models as a registration reference.

Data availability statement

The data that support the findings of this study are openly available at the following URL/DOI: https://doi.org/10.34894/2D0FRT.

Funding Statement

This research was funded by Elekta AB, Stockholm, Sweden.

Acknowledgment

The authors would like to thank Renee Rijnsdorp and Bart Kodde for their help in performing the CT imaging acquisitions.

ORCID iDs

Ioannis Androulakis https://orcid.org/0000-0003-4816-7048
Jeremy Godart https://orcid.org/0000-0001-5070-8128
Robin Straathof https://orcid.org/0000-0002-0396-8880
Henrike Westerveld https://orcid.org/0000-0002-7975-9604
Remi Nout https://orcid.org/0000-0001-8011-2982

Mischa Hoogeman https://orcid.org/0000-0002-4264-9903
Inger-Karine K Kolkman-Deurloo https://orcid.org/0009-0004-8452-3198

References

Androulakis I *et al* 2024 Assessment of integrated electromagnetic tracking for dwell position monitoring in a clinical HDR brachytherapy setting for prostate cancer *Radiother. Oncol.* **200** 110501
Androulakis I 2025 Replication Data for: Afterloader integrated EMT enables improved dwell position model definition and quality assurance in Venezia gynaecological brachytherapy applicators *DataverseNL* (https://doi.org/10.34894/2D0FRT)
Androulakis I, Godart J, Luthart L, Christianen M E M C, Westerveld H, Nout R A, Hoogeman M and Kolkman-Deurloo I-K-K 2025 Reconstruction errors in clinical intraoperative TRUS–based prostate HDR-BT detected using electromagnetic tracking *Brachytherapy* **24** 177–85
Awunor O A, Dixon B and Walker C 2013 Direct reconstruction and associated uncertainties of 192Ir source dwell positions in ring applicators using gafchromic film in the treatment planning of HDR brachytherapy cervix patients *Phys. Med. Biol.* **58** 3207
Awunor O, Berger D and Kirisits C 2015 A multicenter study to quantify systematic variations and associated uncertainties in source positioning with commonly used HDR afterloaders and ring applicators for the treatment of cervical carcinomas *Med. Phys.* **42** 4472–83
Beaulieu L, Racine E, Han D Y, Vigneault E, Hsu I C and Cunha J A M 2018 Real-time electromagnetic tracking–based treatment platform for high-dose-rate prostate brachytherapy: clinical workflows and end-to-end validation *Brachytherapy* **17** 103–10
Bert C, Kellermeier M and Tanderup K 2016 Electromagnetic tracking for treatment verification in interstitial brachytherapy *J. Contemp. Brachytherapy* **8** 448–53
Damato A L, Viswanathan A N, Don S M, Hansen J L and Cormack R A 2014 A system to use electromagnetic tracking for the quality assurance of brachytherapy catheter digitization *Med. Phys.* **41** 101702
Deufel C L, Brost E E, Dupere J M, Petersen I A, Haddock M G and Garda A E 2024 EMVision: an electromagnetic tracking guidance system for accurate placement of interstitial brachytherapy applicators *Brachytherapy* **23** 676–86
DeWerd L A, Ibbott G S, Meigooni A S, Mitch M G, Rivard M J, Stump K E, Thomadsen B R and Venselaar J L M 2011 A dosimetric uncertainty analysis for photon-emitting brachytherapy sources: report of AAPM Task Group No. 138 and GEC-ESTRO *Med. Phys.* **38** 782–801
Dürrbeck C, Gomez-Sarmiento I N, Androulakis I, Sauer B C, Kolkman-Deurloo I K, Bert C and Beaulieu L 2024 A comprehensive quality assurance protocol for electromagnetic tracking in brachytherapy *Med. Phys.* **51** 3184–94
Dürrbeck C, Gulde S, Abu-Hossin N, Fietkau R, Strnad V and Bert C 2022a Influence and compensation of patient motion in electromagnetic tracking based quality assurance in interstitial brachytherapy of the breast *Med. Phys.* **49** 2652–62
Dürrbeck C, Sauer B C, Lotter M, Kreppner S, Strnad V, Fietkau R and Bert C 2022b Automating implant reconstruction in interstitial brachytherapy of the breast: a hybrid approach combining electromagnetic tracking and image segmentation *Radiother. Oncol.* **176** 172–8
Elekta Brachytherapy 2018 Oncentra brachy v4.6–physics and algorithms
Espinoza A, Beeksma B, Petasecca M, Fuduli I, Porumb C, Cutajar D, Corde S, Jackson M, Lerch M L F and Rosenfeld A B 2013 The feasibility study and characterization of a two-dimensional diode array in “magic phantom” for high dose rate brachytherapy quality assurance *Med. Phys.* **40** 111702
Franz A M, Haidegger T, Birkfellner W, Cleary K, Peters T M and Maier-Hein L 2014 Electromagnetic tracking in medicine—a review of technology, validation, and applications *IEEE Trans. Med. Imaging* **33** 1702–25
Gomez-Sarmiento I N, Tho D, Dürrbeck C, de Jager W, Laurendeau D and Beaulieu L 2024 Accuracy of an electromagnetic tracking enabled afterloader based on the automated registration with CT phantom images *Med. Phys.* **51** 799–808
Hellebust T P *et al* 2010 Recommendations from Gynaecological (GYN) GEC-ESTRO Working Group: considerations and pitfalls in commissioning and applicator reconstruction in 3D image-based treatment planning of cervix cancer brachytherapy *Radiother. Oncol.* **96** 153–60
Holschneider C H, Petereit D G, Chu C, Hsu I C, Ioffe Y J, Klopp A H, Pothuri B, Chen L-M and Yashar C 2019 Brachytherapy: a critical component of primary radiation therapy for cervical cancer: from the Society of Gynecologic Oncology (SGO) and the American Brachytherapy Society (ABS) *Brachytherapy* **18** 123–32
Hrinivich W T, Morcos M, Viswanathan A and Lee J 2019 Automatic tandem and ring reconstruction using MRI for cervical cancer brachytherapy *Med. Phys.* **46** 4324–32
Humer I, Kirisits C, Berger D, Trnková P, Pötter R and Nesvacil N 2015 Improved source path localisation in ring applicators and the clinical impact for gynecological brachytherapy *J. Contemp. Brachytherapy* **7** 239–43
Kallis K, Abu-Hossin N, Kreppner S, Lotter M, Strnad V, Fietkau R and Bert C 2019 Estimation of inter-fractional variations in interstitial multi-catheter breast brachytherapy using a hybrid treatment delivery system *Radiother. Oncol.* **141** 312–20
Kallis K, Kreppner S, Lotter M, Fietkau R, Strnad V and Bert C 2018 Introduction of a hybrid treatment delivery system used for quality assurance in multi-catheter interstitial brachytherapy *Phys. Med. Biol.* **63** 095008
Kellermeier M, Herbolzheimer J, Kreppner S, Lotter M, Strnad V and Bert C 2017 Electromagnetic tracking (EMT) technology for improved treatment quality assurance in interstitial brachytherapy *J. Appl. Clin. Med. Phys.* **18** 211–22
Kirisits C *et al* 2014 Review of clinical brachytherapy uncertainties: analysis guidelines of GEC-ESTRO and the AAPM *Radiother. Oncol.* **110** 199–212
Kolkman-Deurloo I *et al* 2022 OC-0278 first clinical results of integrated EMT for quantification of positional deviations in cervix BT *Radiother. Oncol.* **170** S237–S8
Lekatou A, Peppa V, Karaiskos P, Pantelis E and Papagiannis P 2022 On the potential of 2D ion chamber arrays for high-dose rate remote afterloading brachytherapy quality assurance *Phys. Med. Biol.* **67** 085011
Niatsetski Y, Fekkes S and Vreeken H 2011 695 poster source path measurements for ring applicators *Radiother. Oncol.* **99** S278
Otani Y, Sumida I, Nose T, Shimamoto S, Okubo H and Ogawa K 2018 High-dose rate intracavitary brachytherapy pretreatment dwell position verification using a transparent applicator *J. Appl. Clin. Med. Phys.* **19** 428–34

Prisciandaro J et al 2022 AAPM task group report 303 endorsed by the ABS: MRI implementation in HDR brachytherapy—Considerations from simulation to treatment *Med. Phys.* **49** e983–1023

Sauer B C, Dürrbeck C and Bert C 2022 Electromagnetic tracking in interstitial brachytherapy: a systematic review *Front. Phys.* **10** 956983

Sauer B C, Dürrbeck C and Bert C 2024 Electromagnetic tracking for integrated quality assurance in breast interstitial brachytherapy: the impact of registration method *J. Contemp. Brachytherapy* **16** 297–305

Siebert F A, Kirisits C, Hellebust T P, Baltas D, Verhaegen F, Camps S, Pieters B, Kovács G and Thomadsen B 2020 GEC-ESTRO/ACROP recommendations for quality assurance of ultrasound imaging in brachytherapy *Radiother. Oncol.* **148** 51–56

Steenhuijsen J, Harbers M, Hoffmann A, de Leeuw A, Rijnders A and Unipan M 2018 Report 30: code of practice for quality assurance of brachytherapy with Ir-192 afterloaders (Netherlands Commission on Radiation Dosimetry)

Straathof R, Meijaard J P, van Vliet-pérez S M, Kolkman-Deurloo I K K, Nout R A, Heijmen B J M, Wauben L S G L, Dankelman J and van de Berg N J 2024 Multibody dynamic modeling of the behavior of flexible instruments used in cervical cancer brachytherapy *Med. Phys.* **51** 3698–710

Taylor B N and Kuyatt C E 1994 *Guidelines for Evaluating and Expressing the Uncertainty of NIST Measurement Results* (US Department of Commerce, Technology Administration, National Institute of)

van Heerden L, Schiphof-Godart J, Christianen M, Mens J-W, Franckena M, Maenhout M, Hoogeman M and Kolkman-Deurloo I-K 2021 Accuracy of dwell position detection with a combined electromagnetic tracking brachytherapy system for treatment verification in pelvic brachytherapy *Radiother. Oncol.* **154** 249–54

van Wagenberg T, Voncken R, van Beveren C, Berbee M, van Limbergen E, Verhaegen F and Fonseca G P 2024 Time-resolved clinical dose volume metrics, calculations and predictions based on source tracking measurements and uncertainties to aid treatment verification and error detection for HDR brachytherapy—a proof-of-principle study *Phys. Med. Biol.* **69** 135006

Watanabe Y *et al* 2018 Automated source tracking with a pinhole imaging system during high-dose-rate brachytherapy treatment *Phys. Med. Biol.* **63** 145002